

Asymmetric Synthesis
How to cite: *Angew. Chem. Int. Ed.* **2021**, *60*, 10203–10210

International Edition: doi.org/10.1002/anie.202017225

German Edition: doi.org/10.1002/ange.202017225

Crystal Structures and Catalytic Mechanism of L-erythro-3,5-Diaminohexanoate Dehydrogenase and Rational Engineering for Asymmetric Synthesis of β -Amino Acids

Na Liu, Lian Wu, Jinhui Feng, Xiang Sheng,* Jian Li, Xi Chen, Jianjiong Li, Weidong Liu, Jiahai Zhou,* Qiaqing Wu,* and Dunming Zhu*

Abstract: Amino acid dehydrogenases (AADHs) have shown considerable potential as biocatalysts in the asymmetric synthesis of chiral amino acids. However, compared to the widely studied α -AADHs, limited knowledge is available about β -AADHs that enable the synthesis of β -amino acids. Herein, we report the crystal structures of a L-erythro-3,5-diaminohexanoate dehydrogenase and its variants, the only known member of β -AADH family. Crystal structure analysis, site-directed mutagenesis studies and quantum chemical calculations revealed the differences in the substrate binding and catalytic mechanism from α -AADHs. A number of rationally engineered variants were then obtained with improved activity (by 110–800 times) toward various aliphatic β -amino acids without an enantioselectivity trade-off. Two β -amino acids were prepared by using the outstanding variants with excellent enantioselectivity (>99% ee) and high isolated yields (86–87%). These results provide important insights into the molecular mechanism of 3,5-DAHDH, and establish a solid foundation for further design of β -AADHs for the asymmetric synthesis of β -amino acids.

Introduction

β -Amino acids are not only found as essential component in natural compounds with interesting biological properties, but also have emerged as a class of important building blocks for synthetic pharmaceuticals and promising scaffolds in peptide research.^[1] Therefore, both chemical and biocatalytic methods have been developed for the construction of β -amino acid moieties.^[2] Among them, the reductive amination of β -keto or β -hydroxyl carboxylic acids and derivatives represents

an attractive straightforward approach to access β -amino acids and derivatives.^[3] Recently, direct amination of β -hydroxyl acid esters was achieved using a borrowing hydrogen methodology involving cooperative catalysis of a ruthenium catalyst and a Brønsted acid additive.^[4] Biocatalytic reductive amination of β -keto acids has been reported using transaminases, which catalyze the amino transfer from an amino acid or amine to β -keto acids to give optically active β -amino acids.^[5] While this represents a promising method for the preparation of chiral β -amino acids, the efficiency and scope still desire further improvements for practical applications. A paradigm of biocatalytic asymmetric reductive amination of carbonyl group is the α -amino acid or amine dehydrogenase-catalyzed reductive amination of α -keto acids or ketones in the presence of ammonium as amino donor,^[6] that can be coupled with alcohol dehydrogenase-catalyzed oxidation of alcohols to directly convert hydroxyl group to amino group in the enantioselective manner.^[7] For example, the asymmetric synthesis of L-tert-leucine via leucine dehydrogenase (LeuDH)-catalyzed reductive amination of 3,3-dimethyl-2-oxobutanoic acid is a representative case at industrial scale, showing advantages in terms of atomic economy and environmental impact due to the by-products being H₂O and CO₂ when formate dehydrogenase is used for co-factor regeneration and ammonium formate serves as reactant for both enzymatic reactions.^[8] We thus envisioned that β -amino acid dehydrogenase (β -AADH) could serve as a useful biocatalyst for the asymmetric synthesis of chiral β -amino acids.

However, compared to α -amino acid dehydrogenase (α -AADH), the β -counterpart has been much less studied. To the best of our knowledge, the only reported β -AADH is L-

[*] N. Liu, Prof. Dr. J. Feng, Prof. Dr. X. Sheng, Prof. Dr. X. Chen, J. Li, Prof. Dr. W. Liu, Prof. Dr. Q. Wu, Prof. Dr. D. Zhu
 National Engineering Laboratory for Industrial Enzymes and Tianjin Engineering Research Center of Biocatalytic Technology, Tianjin Institute of Industrial Biotechnology, Chinese Academy of Sciences and National Technology Innovation Center for Synthetic Biology
 Tianjin 300308 (China)
 E-mail: shengx@tib.cas.cn
 wu_qq@tib.cas.cn
 zhu_dm@tib.cas.cn

N. Liu, L. Wu, Prof. Dr. J. Feng, J. Li, Prof. Dr. Q. Wu, Prof. Dr. D. Zhu
 University of Chinese Academy of Sciences
 19A Yuquan Road, Beijing 100049 (China)

Prof. Dr. J. Zhou
 CAS Key Laboratory of Quantitative Engineering Biology, Shenzhen Institute of Synthetic Biology, Shenzhen Institutes of Advanced

Technology, Chinese Academy of Sciences
 Shenzhen 518055 (China)

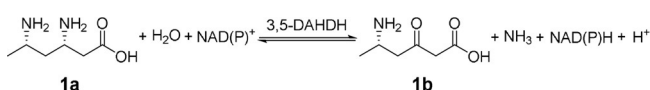
E-mail: jiahai@siat.ac.cn

L. Wu, J. Li, Prof. Dr. J. Zhou
 State Key Laboratory of Bio-organic and Natural Products Chemistry Center for Excellence in Molecular Synthesis, Shanghai Institute of Organic Chemistry, Chinese Academy of Sciences
 Shanghai 200032 (China)

L. Wu
 The Key Laboratory of Synthetic Biology, and CAS Center for Excellence in Molecular Plant Sciences, Institute of Plant Physiology and Ecology, Chinese Academy of Sciences
 Shanghai 200032 (China)

 Supporting information and the ORCID identification number(s) for the author(s) of this article can be found under:
 <https://doi.org/10.1002/anie.202017225>.

erythro-3,5-diaminohexanoate dehydrogenase (3,5-DAHDH, EC.1.4.1.11), which has been identified to participate in the degradation pathway of lysine from some bacterial species.^[9] This NAD(P)H-dependent enzyme catalyzes the reversible deamination/amination reaction between (3*S*,5*S*)-diaminohexanoate (**1a**) and 3-keto-5-amino-hexanoate (**1b**, Scheme 1).^[9a] However, 3,5-DAHDHs exhibited relatively strict substrate specificity toward native substrate **1a**, thus limiting their synthetic applications. In this context, we engineered the 3,5-DAHDH from *Candidatus Cloacamonas acidaminovorans* (3,5-DAHDHcca, Uniprot ID: B0VJ11)^[10] by screening a domain scanning mutagenesis library to broaden the substrate scope.^[11] Although some variants were obtained to show enhanced activities toward several aliphatic and aromatic β -amino acids, little is known about this enzyme and the 3,5-DAHDHs in general.



Scheme 1. *L*-erythro-3,5-Diaminohexanoate dehydrogenase (3,5-DAHDH) catalyzed reaction.

On the other hand, it is still quite a challenge to engineer an enzyme to expand its substrate scope and/or improve its activity while keeping its excellent stereoselectivity. In order to achieve this rational engineering goal, a prerequisite is to understand the catalytic mechanism and substrate-binding of the target enzyme. Herein we report the X-ray crystal structures of 3,5-DAHDHcca and its variants, together with the site-directed mutagenesis and quantum chemical calculations, to reveal the catalytic mechanism of 3,5-DAHDHcca and the molecular basis of substrate specificity, which offered directions for engineering β -AADHs to achieve their synthetic potentials. Subsequently, structure-guided directed evolution of 3,5-DAHDHcca was performed to enhance the activity toward non-native substrates without sacrifice of enantioselectivity, and the obtained variants were applied for the asymmetric synthesis of β -amino acids at preparative scale.

Results and Discussion

Crystal structures of 3,5-DAHDHcca

We solved the structures of 3,5-DAHDHcca in apo form (WT), complexed with cofactor (WT-NADPH), and variant structure E310G/A314Y-NADPH that exhibited a broad substrate-scope in our previous study,^[11] with eight, four and two molecules in the asymmetric unit, respectively (Table S1). Unfortunately, the attempts to obtain the structures bound with amino acid substrate or keto product failed (Section 1.3 in Supporting Information). The overall monomeric structure of 3,5-DAHDHcca was composed of an N-terminal catalytic domain (Domain I) and a C-terminal cofactor-binding domain (Domain II) separating by a deep cleft (Figure 1a), that showed similarities to the structures of α -AADHs and the recently reported native amine dehydrogenases (AmdH) at the single subunit level,^[12] although there was no significant sequence homology between them. The cofactor-binding domain of 3,5-DAHDHcca contained the typical Rossmann fold observed in all NAD(P)H-dependent dehydrogenases,^[13] but the catalytic domain was significantly different from them. The catalytic domain of 3,5-DAHDHcca was featured by six anti-parallel β -strands almost bent into U-shape with two α -helices, while the β -sheets were straight in LeuDH, phenylalanine dehydrogenase (PheDH), *meso*-diaminopimelate dehydrogenase (DAPDH) and AmdH.^[12b-e] In the structures of 3,5-DAHDHcca, every two monomers were packed into a homodimer by hydrogen bond interactions between the cofactor-binding domain of each subunit. The dimerization resulted in 12-stranded β -sheets spanning two molecules in an antiparallel manner as presented in Figure 1a. This is different from the crystal structures of LeuDH, PheDH, DAPDH, and AmdH in which the dimeric architecture is constructed by the β -sheets in catalytic domain rather than the cofactor-binding domain.^[12b-e]

The electron density of WT-NADPH unequivocally revealed that two cofactors were bound on the interface of two monomers (monomer A and C) forming a homodimer with the nicotinamide ring deep in the active cleft (Figure 1b). The ensemble framework of this homodimer binding with NADPH had no significant difference to the ligand-free structure (Figure S1), with a root mean square deviation

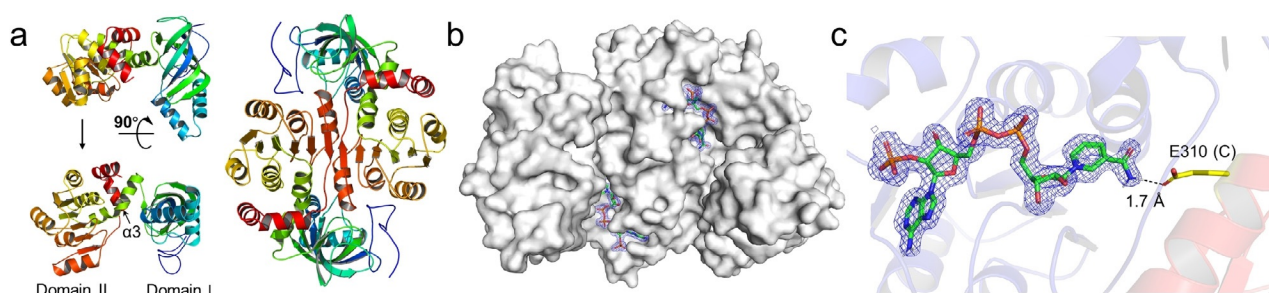


Figure 1. Crystal structures of 3,5-DAHDH from *Candidatus Cloacamonas acidaminovorans* (3,5-DAHDHcca). a) Secondary structure elements of monomer and homodimer in wild-type structure (WT) are shown as cartoon representations. b) Dimer structure with cofactors binding in monomers A and C of WT-NADPH. c) Zoom-in view of the interaction between the amide of NADPH binding in monomer A (blue) and residue E310 in monomer C (red). The cofactors in (b) and (c) are indicated by the simulated annealing omit maps (blue mesh, contoured at 1.0 σ).

(RMSD) value of 0.63 Å for 700 C_α atoms. While a NADPH was mainly bound to the residues of monomer A (Figure S2), the amide group of nicotinamide also interacted with the residue E310 of monomer C by hydrogen bond (Figure 1c). The binding mode of one NADPH shared by two monomers was not formed by crystal packing, indicating that the dimerization event was required for enzymatic catalysis and each homodimer was a minimal integral functional unit. However, in the reported structures of LeuDH, PheDH, DAPDH and native AmDH, the substrate-binding pockets are constructed by one subunit.^[12b–e]

We also compared the structures of WT·NADPH and E310G/A314Y·NADPH. Most obviously, E310G destroyed the hydrogen bond interaction with the amide group of NADPH observed in the wild-type structure. While mutation showed no significant effect on the conformation of cofactor-binding domain, the catalytic domain of the NADPH-bound subunit (monomer B) in E310G/A314Y·NADPH exhibited a tremendous conformational change by the superimposition with monomer A of WT·NADPH (Figure 2a), with an RMSD of 3.89 Å for 352 C_α atoms. Among the α-AADHs, inter-domain flexibility is characterized by the angle of domain cleft.^[12c,14] In 3,5-DAHDHcca, the angle was quantified by three C_α atoms of T91 in Domain I, D177 in the helix α3 at the base of the cleft, and M298 in Domain II. For the structures of 3,5-DAHDHcca in apo state and complexed with NADPH, the angle between two domains ranged from 46.1° to 56.6°, which were observed to be an open form. By contrast, the monomer B in E310G/A314Y·NADPH exhibited a relative closed conformation with a smaller angle of 22.2° (Figure 2a). It is also worth to note that, the ≈30° inter-domain movement enabled the side chains of D49 and S50 to shift about 8.2 Å and 8.8 Å toward NADPH, respectively, resulting in the formation of hydrogen bonds with the nicotinamide ribose and pyrophosphate moiety (Figure 2b). Additionally, the flexibility of catalytic domain was also confirmed by the much higher B-factors of E310G/A314Y·NADPH compared to WT·NADPH (Figure S3). We thus propose that the conformation of E310G/A314Y·NADPH structure is probably closer to the reaction state and the proposed substrate binding pocket indicated by C4 of NADPH is shown in Figure 2c. Considering that the enzyme is dynamic and

allosteric, it is not uncommon that conformation changes are involved in substrate binding and product release.^[15] In the functionally similar NAD(P)H-dependent dehydrogenases, it is also generally believed that the apo state has an open cleft which closes upon the binding of reactants.^[14b]

Active sites and catalytic mechanism of 3,5-DAHDHcca

To understand how 3,5-DAHDHcca recognizes the β-amino acid substrate and cofactor NADP⁺, and the reaction mechanism, quantum chemical calculations^[16] were performed by using a large active site model of the ternary complex (Figure S4) constructed on the basis of the E310G/A314Y·NADPH structure by modifying the two mutated residues back to their original forms. The native substrate **1a** was docked into the active sites. According to the pH dependence of 3,5-DAHDHcca (Figure S5), the oxidative deamination activity toward **1a** increased rapidly under alkaline conditions from pH 9.0, and the optimum pH was 11.0, which is similar to that for some PheDHs and LeuDHs.^[17] Therefore, the titratable residues (D49, D177, K203 and E310) and **1a** in the employed model were set as deprotonated states.

As shown in the optimized structure of the ternary complex (called **E:DAH**, Figure S6), the carboxylate and C5-amino groups of **1a** are captured by the side chains of S125 and E310, respectively. The other amino group at C3 forms two hydrogen bonds with D49 and D177. For NADP⁺, the 2'-hydroxyl of nicotinamide ribose and the amide group interact with D49 and E310, respectively. Some main chain groups are also involved in the binding of **1a** and NADP⁺, including G94, G95, G180, G321 and G323.

In the proposed mechanism (Figure 3), the catalytic cycle starts with the hydride transfer from C3 of **1a** to C4 of NADP⁺ with a barrier of 18.8 kcal mol⁻¹ (**TS1**, Figure S7 for structure). The generated iminium intermediate (**Int1**) is 1.8 kcal mol⁻¹ lower than **E:DAH**. In the next hydration step, both the deprotonated C5-amino group of **1a** and D177 can be the catalytic base to activate the water molecule that attacks the electrophilic carbon of **Int1**. The barrier is 8.3 kcal mol⁻¹ (**TS2**) or 12.4 kcal mol⁻¹ (**TS2'**) relative to **Int1**

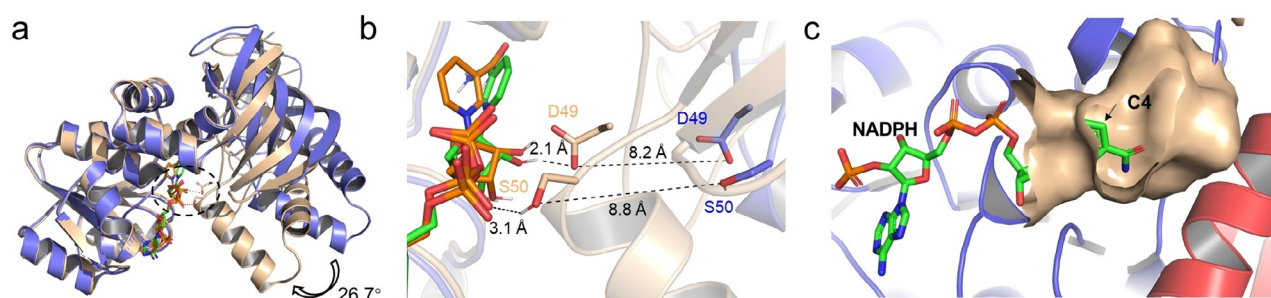


Figure 2. Structural comparison of WT·NADPH and E310G/A314Y·NADPH, and the proposed substrate pocket in E310G/A314Y·NADPH. a) Superimposed overall structures of WT·NADPH monomer A (light blue) and E310G/A314Y·NADPH monomer B (wheat) with an angle of 48.9° and 22.2°, respectively. b) Zoom-in view of the interactions between D49, S50 and NADPH (green in E310G/A314Y·NADPH and orange in WT·NADPH). c) Substrate pocket of E310G/A314Y·NADPH indicated by the coordinate of C4 of NADPH. The substrate pocket was relatively hydrophobic and mainly comprised of residues both from monomer A (red, L307, G310, G311) and B (blue, M96, L123, V124, S125, V159, L176, D177, V178, A179, G180, G323, Y324 and H328).

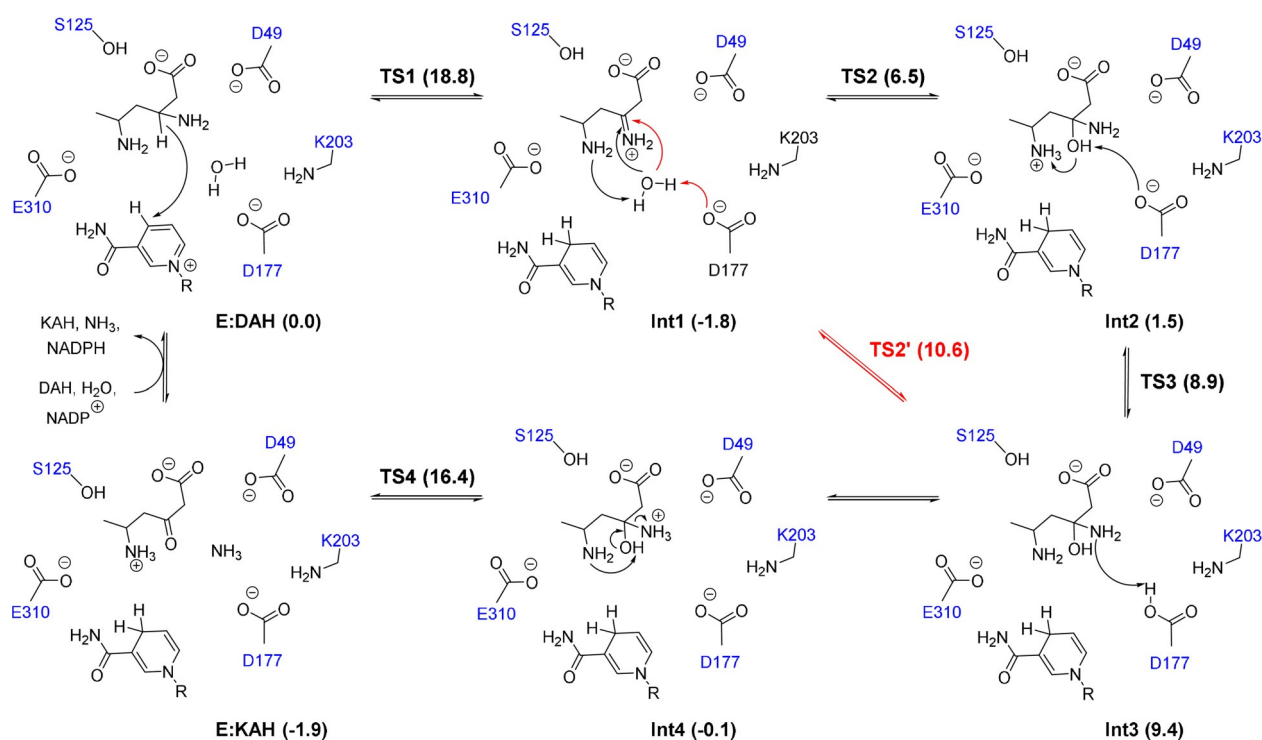


Figure 3. Proposed catalytic mechanism of 3,5-DAHDHcca. The relative energies of all the intermediates and transition states are given in kcalmol⁻¹ in parentheses. Optimized structures for all the intermediates and transition states are given in Figure S7.

for the pathways with C5-amino group or D177, respectively. For the former pathway, after the formation of hydrated intermediate (**Int2**), a proton transfer takes place from the protonated C5-amino group to D177 via the newly formed hydroxyl group with a barrier of 10.7 kcalmol⁻¹ (**TS3**) relative to **Int1**, arriving at the same intermediate (**Int3**) as the latter pathway. Then, a proton transfer from D177 to C3-amino group results in intermediate **Int4** with -0.1 kcalmol⁻¹ energy, in which the protonated amino group can be significantly stabilized by the carboxylate groups of D49 and D177. Finally, the products are formed by the C–N bond cleavage, concurrently with intramolecular proton transfer from the C3-hydroxyl group to the C5-amine (**TS4**). This step has a barrier of 18.2 kcalmol⁻¹ relative to **Int1**. The energy of enzyme-product complex **E:KAH** is 1.9 kcalmol⁻¹ lower than **E:DAH**. In **E:KAH**, the protonated C5-amino is stabilized by the interaction with the side chain of E310.

Both the hydride transfer and the deamination can be rate-limiting steps (RDSs) for 3,5-DAHDHcca, since they have very similar barriers (18.8 kcalmol⁻¹ vs. 18.2 kcalmol⁻¹). The calculated barrier of the overall reaction is in good agreement with the experimentally measured rate constant (k_{cat}) of 553 min⁻¹ (Table S2), corresponding to an activation energy of ca. 16 kcalmol⁻¹ according to classical transition state theory. For α -AADHs that share a similar catalytic mechanism as 3,5-DAHDHcca, their RDSs are still not established.^[6a,18] However, it was proposed that the hydride transfer is unlikely to be RDS for the oxidation reaction of PheDH.^[18c] An interesting finding for 3,5-DAHDHcca is that D177 and the C5-amino group of **1a** could serve as the catalytic group to accept the proton, in favor of the latter by

ca. 2 kcalmol⁻¹. This explained why the wild-type enzyme exhibited a hundreds of times lower activity (10 mUmg⁻¹) toward (*S*)-3-amino-hexanoic acid (**2a**) lacking C5-amino group compared to **1a** (3.0 Umg⁻¹).^[11] These results thus provide the molecular insights into the substrate specificity of 3,5-DAHDHcca toward **1a**.

To further verify the contributions of the above-identified amino acid residues during the catalysis, we performed site-directed mutagenesis and measured the enzymatic activities (Figure 4) and kinetic parameters (Table S2 for **1a**, Table S3 for NADP⁺). Replacement of S125 with alanine resulted in almost loss of the enzyme activity, but S125T showed $\approx 6\%$ activity of the wild-type enzyme, and was ≈ 300 times higher than S125A. The 20-fold increased K_m value of S125A for substrate **1a** and the partial rescue of this almost inactive variant by S125T suggested that the hydroxyl group of this residue is important for the binding of carboxyl group of the substrate, and these results are consistent with the above analysis of the substrate binding mode. All the variants of E310 exhibited much lower activities than the wild-type enzyme for the native substrate **1a**.^[11] And the variant E310G exhibited a ≈ 90 -fold decreased k_{cat} (6.25 min⁻¹) toward **1a**, and two times increased K_m values for both NADP⁺ and **1a**. These results proved that residue E310 was vital for catalysis and substrate recognition since it was bound with the amide of NADPH and the C5-amino group of **1a**. The mutation of S50A did not significantly affect the enzyme activity, and this was supported by the evolutionary analysis that across 831 diverse 3,5-DAHDH sequences this residue was conserved as either serine or alanine at a similar frequency (Figure S8). In contrast, substituting S50 with threonine that possesses the

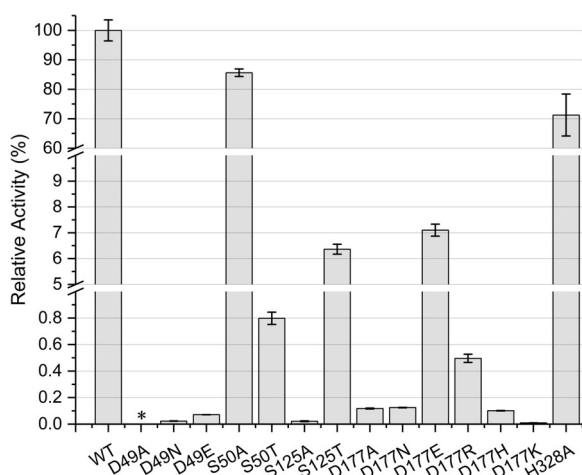


Figure 4. Relative activity of 3,5-DAHDHcca variants for oxidative deamination toward **1a**. The activity of wild-type enzyme was set as 100%. Asterisks indicate that the activity was not measurable. Error bars represent the standard deviations of three replicates.

similar property as serine caused a 100-fold loss of activity, suggesting that the extra methyl group in the side chain might prevent the hydrogen bond interaction between the hydroxyl group with pyrophosphate moiety of NADPH (as shown in Figure 2b) and thus led to a decreased activity. The substitution of residue D49 with alanine led to the complete deactivation, and the activity was less than 0.1% of the wild-type 3,5-DAHDHcca by replacing D49 with N or E. Mutation of D49 to N might not significantly change its hydrogen bond network with the nicotinamide ribose of NADP⁺ and the C3-amino group of **1a**, resulting in only about 1.4-fold and 3.8-fold increase in K_m values toward NADP⁺ and **1a**, respectively, compared to wild-type enzyme. However, variant D49N had a significantly lower ability to stabilize the **Int4** in Figure 3 due to lack of the ionic interaction with C3-NH₃⁺, leading to the catalytic constant k_{cat} dropping 675-fold for **1a**. The removal of carboxyl group at residue D177 was detrimental to enzyme activity, both variants D177A and D177N decreased the activity nearly a thousand times. The K_m value of D177A for **1a** was approximate to that of wild-type, but the k_{cat} was decreased by ≈ 3000 -fold. In addition, the enzyme activity could be restored to $\approx 7\%$ of the wild-type enzyme by D177E which also has a carboxyl group but one methylene longer than aspartic acid, indicating that the carboxyl group at this position may play a key role in the catalytic process and the length of amino acid side chain also has an important effect on catalysis. These results are consistent with the proposed catalytic mechanism (Figure 3) that D177 serves as a catalytic residue being involved in the proton transfer with C3-NH₂ group of the substrate, rather than a role of binding (recognition) substrate. For the DAPDHs and native AmDHs, D or E is also proposed as the key catalytic residue.^[12e,14c] In the catalytic mechanism of LeuDH and PheDH, lysine is the catalytic residue participated in the hydration step of the deamination direction.^[18b,c] However, for 3,5-DAHDHcca, the activity of the variant D177K was barely detected, and the enzyme activities of D177R and D177H were less than 1% that of wild-type

enzyme. In addition, replacement of the only basic residue H328 in the active sites of 3,5-DAHDHcca with alanine did not significantly affect the activity, suggesting that it was not essential for the enzyme function. Overall, the site-directed mutagenesis studies confirmed the likely roles of these specific residues of 3,5-DAHDHcca, that showed some differences from α -AADHs.

Structure-guided directed evolution of 3,5-DAHDHcca for non-native substrates

Although 3,5-DAHDHs offer a new venue for the asymmetric synthesis of β -amino acids, it is limited due to their quite strict substrate specificity. In previous work by screening 85 variant libraries of 3,5-DAHDHcca, we identified variants E310G/A314Y and E310S/A314N with improved activities toward (*R*)- β -homomethionine (**3a**) by ≈ 200 times. Further mutagenesis studies showed that the replacement of E310 rather than A314 significantly affected the substrate scope.^[11] This is consistent with the substrate binding mode that the C5-amino group of the native substrate interacts with the carboxyl group of E310. Therefore, further engineering of 3,5-DAHDHcca to enhance the activity toward β -amino acids was performed on the basis of variant E310G.

The crystal structures of 3,5-DAHDHcca and the optimized ternary complex **E:DAH** indicated that the substitution of E310 with glycine would destroy its binding with the amide of NADPH. The optimized structure of enzyme-substrate (**3a**) complex for the E310G variant further revealed a flip of the amide group due to the absence of a hydrogen bond with E310 (Figure S9). As such, we hypothesized that the catalytic activity of this enzyme could be improved by reconstructing this interaction between the amide group of NADPH and nearby residues. The E310G/A314Y-NADPH structure showed that the residues within a 4 Å radius sphere centered on the C-atom of amide included F296, M298 and G323 (Figure S10). Due to the direct π - π interaction between F296 with the nicotinamide ring of NADPH, F296 was excluded from mutation. The side chain of M298 was located in the side of nicotinamide ring of NADPH that is away from the amide, this residue was not considered for mutation either. Considering that the C α atom of G323 was only 3.8 Å away from the amide group of NADPH, it was firstly replaced with serine that has a shortest side chain with a hydroxyl group. The result showed that variant E310G/G323S improved the specific activity toward **3a** by 17-fold compared to variant E310G (Table S4). Furthermore, the enzyme activity of E310G/G323T was increased by 5 times toward **3a** (Table S4), which proved the importance of the hydroxyl on this residue. The kinetic data showed that E310G/G323S had slight lower K_m toward NADP⁺ (13.0 μ M vs. 16.9 μ M, Table S3) and **3a** (30.4 mM vs. 40.5 mM, Table S5) compared to E310G. The structures of E310G/G323S-NADPH and E310G/A314Y-NADPH (Table S1) indicated that the substitution of G323 with serine may introduce an additional hydrogen bond between the hydroxyl side chain of S323 and the amide group of NADPH

(Figure S11). This interaction was corroborated by quantum chemical calculations on the enzyme-substrate (**3a**) complex of E310G/G232S variant (Figure S12). Moreover, the comparison between the optimized structures of E310G and E310G/G232S variants showed that there was no significant difference in the binding mode of **3a**.

Subsequently, the substrate binding pocket was modified to better accommodate R-groups of aliphatic substrates by using **3a** as a model substrate. Subsequent mutagenesis was carried out using E310G/G232S as the starting chassis. Three site-directed saturation mutagenesis libraries of residues L123, A179 and H328 locating around the R-group of **3a** (as shown in Figure S12) were constructed and screened against substrate **3a**. The substitution of L123 did not enhance the enzyme activity toward **3a**. When A179 was substituted with S, V, T or C, or H328 was substituted with S, V, T or F, the activity was enhanced by 2–3 times, and E310G/G232S/H328N exhibited the highest activity (5.1 U mg^{-1}) that was 4.6 times relative to E310G/G232S (Table S4). Next, the combinatorial mutagenesis was performed by the replacement of A179 with S, V, T and C on the basis of E310G/G232S/H328N, which further enhanced the activities toward **3a** by 14–145% compared to E310G/G232S/H328N. The best combinatorial variant A179S/E310G/G232S/H328N exhibited a ≈ 200 times enhanced activity (Figure 5), and the lower K_m value compared to E310G/G232S (14.3 mM vs. 30.4 mM, Table S5) suggested a higher affinity toward **3a**. The $> 10^4$ -fold increased activity compared to wild-type of 3,5-DAHDHcca toward non-native substrate **3a** indicated a great potential of protein engineering for this enzyme.

β -Homologous amino acids are a class of valuable building blocks for novel analogues of bioactive peptides.^[19] Therefore, the substrate scope of A179S/E310G/G232S/H328N was tested toward various β -homologous amino acids (Table S6). The results showed that this variant had good activities toward aliphatic substrates **2a** and (*S*)- β -homolysine (**4a**) with a $> 10^2$ -fold increase compared to E310G, except the activity toward (*S*)- β -aminobutyric acid (**5a**) was enhanced to about 6 times. For aromatic substrates, the activity of A179S/E310G/G232S/H328N toward (*R*)- β -phenylalanine

(**6a**) was increased by 2.2 times relative to E310G. And it extended the substrate scope to (*S*)- β -homophenylalanine (**7a**), although the activity was only 5.3 mU mg^{-1} . The activity toward (*R*)- β -homoserine (**8a**) was not enhanced, and this variant did not show measurable activity toward (*S*)- β -homotyrosine (**9a**), (*S*)- β -homoglutamic acid (**10a**) and (*S*)- β -homoglutamine (**11a**). These results demonstrated that the structure-guided mutagenesis of 3,5-DAHDHcca give ready access to enzyme variants for the target β -amino acids although further expansion of the substrate scope is required.

Asymmetric preparation of chiral β -amino acids

To evaluate the feasibility of the biocatalytic reductive amination using these enzyme variants for the synthesis of β -amino acids, the reductive aminations of the β -keto acids 5-(methylthio)-3-oxopentanoic acid (**3b**) and 3-ketohexanoic acid (**2b**) were scaled up to 30 mL to prepare **3a** and **2a**, respectively. These β -keto acids were obtained by hydrolyzing the corresponding β -keto esters with Novozym 435. Since β -keto acids decompose easily in aqueous solution, the fed-batch method was applied for the substrate loading and the final substrate concentration was up to $\approx 154 \text{ mM}$. The recombinant *E. coli* cells overexpressing variant A179S/E310G/G232S/H328N or E310G/G232S/H328N were used as the biocatalysts and freeze-dried D-glucose dehydrogenase (GDH) from *Bacillus subtilis* was used for the cofactor recycling.

The preparation of **3a** was carried out using the most efficient variant A179S/E310G/G232S/H328N, achieving 93% analytical yield in 4 h (Figure S13) with $ee > 99\%$ (Figure S14). For the synthesis of **2a**, we speculated that the substitution of A179 with serine in A179S/E310G/G232S/H328N may be unfavorable for the hydrophobic substrate **2a**. Indeed, the variant E310G/G232S/H328N had higher oxidative deamination activity (5.7 U mg^{-1}) toward **2a** than A179S/E310G/G232S/H328N (2.0 U mg^{-1}). The reductive amination of **2b** was thus performed by using variant E310G/G232S/H328N. As shown in Figure S15 and Figure S16, **2a** was obtained at 95% analytical yield in 4 h with $ee > 99\%$. The optically pure products were isolated in 86% (**3a**) and 87% (**2a**) yields, respectively (Figure S17 and Figure S18). Therefore, these engineered β -AADHs showed great potential as biocatalysts for the asymmetric synthesis of the target β -amino acids.

Conclusion

The crystal structures of 3,5-DAHDHcca show that the catalytic domain is significantly different from that of α -AADHs.^[12] The binding mode of one NADPH shared by two monomers indicates that the substrate pocket of 3,5-DAHDHcca is constructed by homodimer, while each monomer of α -AADHs is a catalytic unit.^[12b-d] The subsequent quantum chemical calculations and mutagenesis studies provide valuable insight into the substrate binding mode and catalytic mechanism of 3,5-DAHDHcca. It was shown that

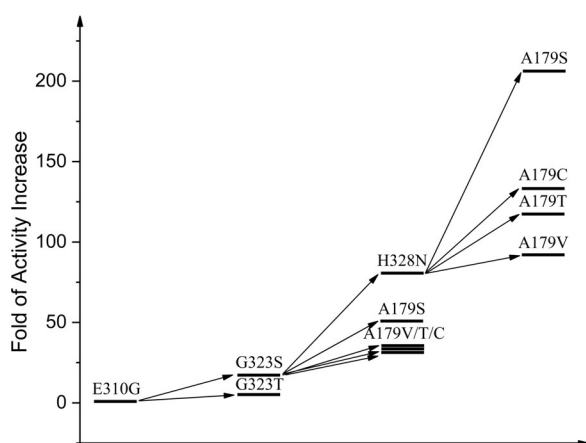


Figure 5. The iterative stepwise improvement process of directed evolution of 3,5-DAHDHcca toward substrate **3a**. Enzyme activity of E310G was taken as 1.0.

D49, E310 and S125 contribute to the binding of the C3-amino, C5-amino and carboxyl groups of the native substrate **1a**, respectively. Moreover, residues D49 and E310 also play important roles in capturing the 2'-hydroxyl of nicotinamide ribose and the amide group of NADPH, respectively. The oxidative deamination reaction of 3,5-DAHDHcca consists of hydride transfer, the successive formation of iminium and hydrated intermediates, and the final cleavage of C–N bond. Although this is similar to that of α -AADHs,^[6a,18] an interesting finding of 3,5-DAHDHcca is that both the deprotonated C5-amino group of **1a** and the active site residue D177 can be the proton acceptor to activate the water in the hydration step. The calculations also showed that both the hydride transfer and C–N cleavage steps are rate-limiting. The X-ray and optimized structures further guided the rational engineering of 3,5-DAHDHcca starting from E310G that has been shown with an expanded substrate scope.^[11] The highly efficient variant A179S/E310G/G323S/H328N was obtained by reconstructing the hydrogen bond interaction of the amide of NADPH with nearby residue S323 and subsequently reshaping the substrate pocket. This variant exhibits a \approx 200-fold increased activity toward **3a** compared to E310G, that is \approx 10⁴-fold compared to the wild-type enzyme. It also displays enhanced activities toward other aliphatic substrates such as **2a** and **4a** by $>$ 100-fold compared to E310G. For **2a**, another variant E310G/G323S/H328N exhibited even \approx 3 times higher activity than A179S/E310G/G323S/H328N. Finally, the synthetic abilities of these two outstanding β -AADH variants were established by the successful preparation of **2a** and **3a** with high analytical yields (93%–95%) and excellent enantioselectivity ($>$ 99% ee). It is notable that the rational engineering enabled the substrate scope expansion without trade-off of the stereoselectivity, an on-going challenge in enzyme engineering.

This study not only extends our understanding of the substrate binding and catalytic mechanism of 3,5-DAHDHcca, the first characterized member of β -AADHs, but also shows the potential of this engineered β -AADH in the asymmetric synthesis of β -amino acids and lays the foundation for further rational design of this enzyme to achieve the asymmetric synthesis of target β -amino acids.

Acknowledgements

The work was financially supported by the National Natural Science Foundation of China (Grant Nos. 21778072 and 92056101) to D.Z., Tianjin Synthetic Biotechnology Innovation Capacity Improvement Project (TSBICIP-KJGG-001) to Q.W., the National Key Research and Development Program of China (2019YFA09005000 and 2018YFA0901900) to J.Z. The authors also thank the staff of beamlines BL18U1 and BL19U1 in Shanghai Synchrotron Radiation Facility for access and help with the X-ray data collection.

Conflict of interest

The authors declare no conflict of interest.

Keywords: asymmetric synthesis · biocatalysis · catalytic mechanism · protein engineering · β -amino acid dehydrogenase

- [1] a) F. Kudo, A. Miyanaga, T. Eguchi, *Nat. Prod. Rep.* **2014**, *31*, 1056–1073; b) C. Cabrele, T. A. Martinek, O. Reiser, L. Berlicki, *J. Med. Chem.* **2014**, *57*, 9718–9739; c) R. W. Cheloha, T. Watanabe, T. Dean, S. H. Gellman, T. J. Gardella, *ACS Chem. Biol.* **2016**, *11*, 2752–2762; d) L. Kiss, I. M. Mándity, F. Fülöp, *Amino Acids* **2017**, *49*, 1441–1455; e) A. Henninot, J. C. Collins, J. M. Nuss, *J. Med. Chem.* **2018**, *61*, 1382–1414; f) V. K. Outlaw, D. F. Kreidler, D. Stelitano, M. Porotto, A. Moscona, S. H. Gellman, *ACS Infect. Dis.* **2020**, *6*, 2017–2022; g) T. Katoh, T. Sengoku, K. Hirata, K. Ogata, H. Suga, *Nat. Chem.* **2020**, *12*, 1081–1088.
- [2] a) J.-A. Ma, *Angew. Chem. Int. Ed.* **2003**, *42*, 4290–4299; *Angew. Chem.* **2003**, *115*, 4426–4435; b) A. Liljebblad, L. T. Kanerva, *Tetrahedron* **2006**, *62*, 5831–5854; c) B. Weiner, W. Szymański, D. B. Janssen, A. J. Minnaard, B. L. Feringa, *Chem. Soc. Rev.* **2010**, *39*, 1656–1691; d) M. Ashfaq, R. Tabassum, M. M. Ahmad, N. A. Hassan, H. Oku, G. Rivera, *Med. Chem.* **2015**, *5*, 295–305; e) H. Noda, M. Shibasaki, *Eur. J. Org. Chem.* **2020**, 2350–2361; f) R. Li, H. J. Wijma, L. Song, Y. Cui, M. Otzen, Y. Tian, J. Du, T. Li, D. Niu, Y. Chen, J. Feng, J. Han, H. Chen, Y. Tao, D. B. Janssen, B. Wu, *Nat. Chem. Biol.* **2018**, *14*, 664–670; g) F. Parmeggiani, N. J. Weise, S. T. Ahmed, N. J. Turner, *Chem. Rev.* **2018**, *118*, 73–118; h) N. J. Turner, *Curr. Opin. Chem. Biol.* **2011**, *15*, 234–240.
- [3] a) Q. Yin, Y. Shi, J. Wang, X. Zhang, *Chem. Soc. Rev.* **2020**, *49*, 6141–6153; b) K. Murugesan, T. Senthamarai, V. G. Chandrasekhar, K. Natte, P. C. J. Kamer, M. Beller, R. V. Jagadeesh, *Chem. Soc. Rev.* **2020**, *49*, 6273–6328; c) T. Irrgang, R. Kempe, *Chem. Rev.* **2020**, *120*, 9583–9674.
- [4] A. Afanasenko, T. Yan, K. Barta, *Commun. Chem.* **2019**, *2*, 127.
- [5] a) S. Mathew, H. Bea, N. S. Prabhu, T. Chung, H. Yun, *J. Biotechnol.* **2015**, *196*, 1–8; b) S. Mathew, S.-S. Jeong, T. Chung, S.-H. Lee, H. Yun, *Biotechnol. J.* **2016**, *11*, 185–190; c) S. Mathew, S. P. Nadarajan, U. Sundaramoorthy, H. Jeon, T. Chung, H. Yun, *Biotechnol. Lett.* **2017**, *39*, 535–543; d) G.-H. Kim, H. Jeon, T. P. Khobragade, M. D. Patil, S. Sung, S. Yoon, Y. Won, S. Sarak, H. Yun, *ChemCatChem* **2019**, *11*, 1437–1440; e) X. Feng, J. Guo, R. Zhang, W. Liu, Y. Cao, M. Xian, H. Liu, *ACS Omega* **2020**, *5*, 7745–7750; f) I. Slabu, J. L. Galman, R. C. Lloyd, N. J. Turner, *ACS Catal.* **2017**, *7*, 8263–8284.
- [6] a) M. Sharma, J. Mangas-Sanchez, N. J. Turner, G. Grogan, *Adv. Synth. Catal.* **2017**, *359*, 2011–2025; b) Y.-P. Xue, C.-H. Cao, Y.-G. Zheng, *Chem. Soc. Rev.* **2018**, *47*, 1516–1561.
- [7] F. G. Mutti, T. Knaus, N. S. Scrutton, M. Breuer, N. J. Turner, *Science* **2015**, *349*, 1525–1529.
- [8] a) A. S. Bommarius, K. Drauz, W. Hummel, M. R. Kula, C. Wandrey, *Biocatalysis* **1994**, *10*, 37–47; b) U. Kragl, W. Kruse, W. Hummel, C. Wandrey, *Biotechnol. Bioeng.* **1996**, *52*, 309–319; c) U. Kragl, D. Vasic-Racki, C. Wandrey, *Bioprocess Eng.* **1996**, *14*, 291–297.
- [9] a) J. J. Baker, I. Jeng, H. A. Barker, *J. Biol. Chem.* **1972**, *247*, 7724–7734; b) S. L. Hong, H. A. Barker, *J. Biol. Chem.* **1973**, *248*, 41–49; c) J. J. Baker, C. van der Drift, *Biochemistry* **1974**, *13*, 292–299; d) H. A. Barker, J. M. Kahn, L. Hedrick, *J. Bacteriol.* **1982**, *152*, 201–207; e) H. A. Barker, J. M. Kahn, S. Chew, *J. Bacteriol.* **1980**, *143*, 1165–1170; f) A. Kreimeyer, A.

- Perret, C. Lechaplais, D. Vallenet, C. Médigue, M. Salanoubat, J. Weissenbach, *J. Biol. Chem.* **2007**, *282*, 7191–7197.
- [10] E. Pelletier, A. Kreimeyer, S. Bocs, Z. Rouy, G. Gyapay, R. Chouari, D. Rivière, A. Ganesan, P. Daegelen, A. Sghir, G. N. Cohen, C. Médigue, J. Weissenbach, D. L. Paslier, *J. Bacteriol.* **2008**, *190*, 2572–2579.
- [11] D. Zhang, X. Chen, R. Zhang, P. Yao, Q. Wu, D. Zhu, *ACS Catal.* **2015**, *5*, 2220–2224.
- [12] a) P. J. Baker, K. L. Britton, P. C. Engel, G. W. Farrants, K. S. Lilley, D. W. Rice, T. J. Stillman, *Proteins Struct. Funct. Genet.* **1992**, *12*, 75–86; b) P. J. Baker, A. P. Turnbull, S. E. Sedelnikova, T. J. Stillman, D. W. Rice, *Structure* **1995**, *3*, 693–705; c) G. Scapin, S. G. Reddy, J. S. Blanchard, *Biochemistry* **1996**, *35*, 13540–13551; d) J. L. Vanhooke, J. B. Thoden, N. M. W. Brunhuber, J. S. Blanchard, H. M. Holden, *Biochemistry* **1999**, *38*, 2326–2339; e) O. Mayol, K. Bastard, L. Beloti, A. Frese, J. P. Turkenburg, J. L. Petit, A. Mariage, A. Debar, V. Pellouin, A. Perret, V. de Berardinis, A. Zaparucha, G. Grogan, C. Vergne-Vaxelaire, *Nat. Catal.* **2019**, *2*, 324–333.
- [13] A. M. Lesk, *Curr. Opin. Struct. Biol.* **1995**, *5*, 775–783.
- [14] a) T. Oliveira, S. Panjkar, J. B. Carrigan, M. Hamza, M. A. Sharkey, P. C. Engel, A. R. Khan, *J. Struct. Biol.* **2012**, *177*, 543–552; b) T. Oliveira, M. A. Sharkey, P. C. Engel, A. R. Khan, *Acta Crystallogr. Sect. F* **2016**, *72*, 462–466; c) W. Liu, Z. Li, C.-H. Huang, R.-T. Guo, L. Zhao, D. Zhang, X. Chen, Q. Wu, D. Zhu, *ChemBioChem* **2014**, *15*, 217–222.
- [15] T. C. Pochapsky, S. S. Pochapsky, *Acc. Chem. Res.* **2019**, *52*, 1409–1418.
- [16] a) X. Sheng, M. Kazemi, F. Planas, F. Himo, *ACS Catal.* **2020**, *10*, 6430–6449; b) F. Himo, *J. Am. Chem. Soc.* **2017**, *139*, 6780–6786; c) M. R. A. Blomberg, T. Borowski, F. Himo, R.-Z. Liao, P. E. M. Siegbahn, *Chem. Rev.* **2014**, *114*, 3601–3658.
- [17] a) E. Omidinia, A. Samadi, H. Taherkhani, S. Khatami, N. Moazami, R. R. Pouraie, Y. Asano, *World J. Microbiol. Biotechnol.* **2002**, *18*, 593–597; b) Y. Zhao, T. Wakamatsu, K. Doi, H. Sakuraba, T. Ohshima, *J. Mol. Catal. B Enzym.* **2012**, *83*, 65–72; c) W. Zhu, Y. Li, H. Jia, P. Wei, H. Zhou, M. Jiang, *Biotechnol. Lett.* **2016**, *38*, 855–861.
- [18] a) J. E. Rife, W. W. Cleland, *Biochemistry* **1980**, *19*, 2328–2333; b) T. Sekimoto, T. Matsuyama, T. Fukui, K. Tanizawa, *J. Biol. Chem.* **1993**, *268*, 27039–27045; c) N. M. W. Brunhuber, J. B. Thoden, J. S. Blanchard, J. L. Vanhooke, *Biochemistry* **2000**, *39*, 9174–9187.
- [19] S. Liu, S. H. Gellman, *J. Org. Chem.* **2020**, *85*, 1718–1724.

Manuscript received: December 28, 2020

Revised manuscript received: February 2, 2021

Accepted manuscript online: February 24, 2021

Version of record online: March 24, 2021